4.3 Effects of B, C, N, O, P AND S Impurities on Tungsten Σ27[110]{552} and Σ3[110]{112} Grain Boundaries — W. Setyawan and R. J. Kurtz (Pacific Northwest National Laboratory)

OBJECTIVE

The objective of this research is to support the design of tungsten-based materials with increased fracture resistance using first-principles computational methods.

SUMMARY

Density functional theory was employed to investigate the effects of B, C, N, O, P and S impurities on the properties of W Σ27[110]{552} and Σ3[110]{112} grain boundaries (GBs). Careful search of interstitial sites near the interfaces resulted in 19 and 9 unique interstices in Σ27 and Σ3 respectively. By using the segregation energy as a weighing factor, the average intergranular fracture energies were calculated. It was found that B, C, N and P increase the cohesion of Σ27 by 10.1, 8.9, 4.1 and 2.5% respectively, while O (0.6%) and S (2.7%) embrittle the GB. In Σ3, only C was found to strengthen the interface by 1.2%, while B, N, O, P and S decrease the intergranular cohesion by 1.7, 1.6, 11.2, 18.4 and 19.4% respectively. The impurity content in this study was 1.37 atoms/nm^2.

PROGRESS AND STATUS

Introduction

The development of novel W-based materials that are suitable for future fusion reactors is likely to involve synergistic advancements in intrinsic W alloys [1, 2], grain boundary (GB) engineering [3, 4] and W-based composites [5, 6]. In all of these areas, understanding and controlling the characteristics of materials at intergranular regions are important. Using first-principles methods, we have recently started to study more closely the effects of impurities on the GB cohesion in tungsten. In particular, Σ27a[110]{552} and Σ3a[110]{112} were used to model the high- and low-angle interfaces. We performed careful search of interstitial sites near the interface for each GB. In this article, we report the results for B, C, N, O, P and S impurities.

Formalism

The GB structures were initially relaxed using classical molecular dynamics (MD) utilizing the Finnis-Sinclair type of interatomic potential developed by Ackland and Thetford [7]. Systematic interfacial shifts and atoms relaxations were done to achieve the most stable configurations. The structures obtained from the MD were further optimized via an *ab initio* method. VASP software was used to perform the quantum mechanical calculations based on the plane-wave density functional theory (DFT). Accurate projector-augmented-wave pseudopotentials with Perdew-Burke-Ernzerhof exchange correlations were employed [8–10]. The number of valence electrons for W, B, C, N, O, P and S is 6, 3, 4, 5, 6, 5 and 6 with plane-wave energy cutoff of 223.1, 318.6, 400.0, 400.0, 400.0, 270.0 and 280.0 eV, respectively. The calculations were done using Monkhorst-Pack **k**-points grid of 5×5×1. These settings were needed to achieve convergence < 1 meV.

RESULTS

The necessary slab thickness for the DFT calculations was determined from the convergence tests of the {552} and {112} surface energies, namely 62 layers for the Σ27 and 23 layers for the Σ3 [11]. Figure 1 shows the relaxed structure of the GBs. For Σ27, the dimensions of the simulation cell converged to 8.2, 8.9 and 50.1 Å along x, y and z respectively. The thickness of the 62 {552}-layers was 26.7 Å, leaving enough vacuum to ensure no interaction between the free surfaces. For Σ3, the simulation cell converged to 8.2, 8.9 and 50.1 Å along x, y and z respectively. The thickness of the 23 {112}-layers was 29.6 Å. In Figure 1, the atoms are arranged in two alternating layers along [110] (-y). Tungsten atoms are plotted in dark or light gray depending on which layer they reside. The simulation cell of both GBs contains four such layers for a total of 124 W atoms (Σ27) and 138 W atoms (Σ3). Periodic boundaries were applied along x and y.

Initially, the set of interstitial voids (interstices) was determined within 3.5 Å from the GB plane. Nineteen unique interstices were found. For the Σ3, nine unique interstices were found. In Figure 1, the interstices are shown in small red spheres and labeled based on the nearest-neighbor distance r_{nn} with interstice 1 having the shortest r_{nn}. Two additional interstices labeled *oct* and *tet* are shown near atom *U*. They represent bulk-like interstices possessing octahedral and tetrahedral coordination. The *oct* interstice is located behind atom *U* and midway between atoms *V*.

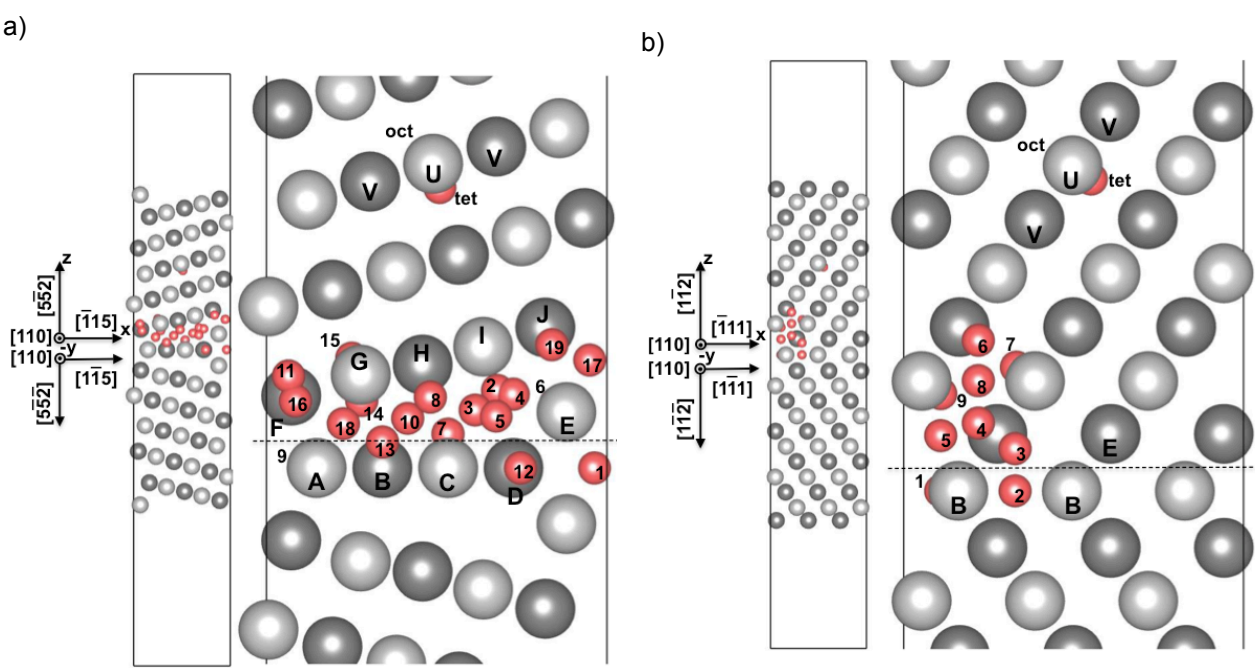

Figure 1. a) Structure of the W Σ27a[110]{552} tilt GB viewed along the [110] (-y). The initial positions of interstices are shown in red spheres from 1 to 19. Interstices 6 and 9 are located behind atoms *E* and *A* respectively. Interstice with octahedral coordination (*oct*) is behind atom *U* midway between atoms *V*. Interstice with tetrahedral coordination is labeled as *tet*. B) Structure of the W Σ3a[110]{112} tilt GB and the positions of interstices labeled from 1 to 9.

For the determination of the GB segregation energy E_{sg}, a reference site needs to be determined. For each impurity, the reference site is determined from the more stable site between *oct* and *tet* sites. The impurity binding energy E_b and GB segregation energy E_{sg} were defined as:

$$E_b = E - (E_W + E_I) \quad (1)$$
$$E_{sg} = E_{ref} - E \quad (2)$$

E denotes the total energy of the system with an impurity at an interstice, E_W is the total energy with only W atoms, E_I is the energy of an isolated impurity, E_{ref} is the total energy with an impurity at the reference site. The interstitial binding energies in body-centered cubic (bcc) W are presented in Table 1. Negative E_b represents an attractive interaction. Boron, C, N and O are attracted to W while P and S are repelled. Carbon is the most binding, followed by N, O and B. For all impurities in this study, *oct* is more stable than *tet* ($E_{ref} = E_{oct}$) except for O ($E_{ref} = E_{tet}$). With these references, the segregation energy at each GB interstice was calculated and summarized in Table 2. Positive values indicate tendency for segregation to the interface. Strong tendencies were observed for all the impurities considered here, particularly in Σ27. Despite the fact that B, C, N and O exhibit strong binding in bcc, their GB segregation energies are large ranging from approximately 1 to 3.5 eV. Meanwhile, as expected, P and S exhibit the largest segregation energy due to their repulsive nature with W atom with the segregation energies ranging from approximately 1 to 8.5 eV.

Table 1. Binding energy E_b (eV) of impurities at octahedral (*oct*) and tetrahedral (*tet*) interstitial site in bcc W. Negative value indicates attraction.

	B	C	N	O	P	S
oct	**-5.107**	**-8.399**	**-8.091**	-5.120	**0.393**	**1.588**
tet	-3.522	-6.897	-7.326	**-5.396**	0.529	1.738

Table 2. Segregation energy E_{sg} (eV) of impurities at various interstices in W Σ27 and Σ3 GBs. Positive E_{sg} indicates tendency to segregate to the GB.

Σ27	1	2	3	4	5	6	7	8	9	10
B	2.206	3.575	3.575	3.576	3.575	3.569	3.577	3.606	2.260	3.545
C	2.115	2.688	2.687	2.688	2.687	2.846	2.683	1.955	0.769	1.966
N	2.176	2.721	2.719	2.721	2.720	3.311	2.714	2.296	1.514	2.297
O	2.109	2.973	3.282	2.973	3.282	3.612	3.038	2.629	1.776	2.635
P	5.788	7.700	7.702	7.700	7.703	7.697	8.226	7.704	5.783	7.689
S	5.211	6.958	6.865	6.958	6.885	6.554	7.090	6.869	5.212	6.722
	11	12	13	14	15	16	17	18	19	
B	2.177	0.226	1.659	3.643	3.242	2.169	3.656	0.986	0.430	
C	2.148	0.456	1.054	3.118	3.113	2.148	1.646	1.117	0.509	
N	2.129	1.185	1.524	1.287	3.145	2.131	2.920	1.290	0.619	
O	3.446	1.645	2.636	1.947	2.962	3.448	3.449	1.958	3.448	
P	8.118	2.657	4.587	8.031	8.038	8.392	8.347	8.123	8.382	
S	7.113	3.128	6.861	7.196	7.203	8.040	8.002	7.091	8.009	
Σ3	**1**	**2**	**3**	**4**	**5**	**6**	**7**	**8**	**9**	
B	1.506	1.507	1.540	1.541	0.681	0.171	0.334	0.672	0.683	
C	1.562	1.562	1.569	1.566	0.642	0.188	0.039	0.648	0.636	
N	1.720	1.717	1.723	1.723	-0.334	0.247	0.432	0.684	0.671	
O	1.807	1.228	0.737	0.471	0.780	0.190	0.339	0.903	0.323	
P	2.908	2.915	3.030	3.026	2.906	0.127	0.838	1.618	0.806	
S	2.896	2.895	3.033	2.994	3.006	0.258	0.861	1.587	0.874	

The effect of impurities on the GB cohesion was studied by calculating the intergranular fracture energy E_{if} as follows:

$$E_{if} = E_{top} + E_{bot} - E \tag{3}$$

$$\Delta E_{if} = E_{if} - E_{if,clean} \tag{4}$$

$$\left\langle E_{if} \right\rangle = \left(\sum_{E_{sg,i}>0} E_{sg,i} E_{if,i} \right) / \sum_{E_{sg,i}>0} E_{sg,i} \tag{5}$$

$$\Delta \left\langle E_{if} \right\rangle = \left\langle E_{if} \right\rangle - E_{if,clean} \tag{6}$$

To obtain the fractured configurations, the system was separated into two subsystems containing atoms below (for the bottom half) or above (for the top half) the fracture plane (dash line in Figure 1). E_{top} and E_{bot} are the total energies of the top and bottom halves respectively. $E_{if,clean}$ denotes the fracture energy of the clean Σ27 (4.16 J/m^2) or Σ3 (6.18 J/m^2). As a first approximation, a measure of an average fracture energy $\langle E_{if} \rangle$ was introduced by using the segregation energy as a weighing factor. Only interstices with $E_{seg} > 0$ were included in the summation. In this formulation, if an impurity is more stable at the bulk than at a GB interstice, then its contribution at this interstice is zero as would be expected.

Figure 2 shows the distribution of E_{if}. The horizontal lines mark the intergranular fracture energies of the clean GBs. The influence of impurities significantly depends on the interstices as evident from Figure 2. The ranges of the $\Delta E_{if}/E_{if,clean}$ are summarized in Table 3 and given in percentage. In general, the impurities affect the GB cohesion more adversely in low-angle GBs than in high-angle ones. Note that in this study, both GBs have the same interface area; hence the comparison is based on the same impurity content of 1.37 atoms/nm^2. From the average values, it was indicated that B, C, N and P increases the cohesion of Σ27 by 10.1, 8.9, 4.1 and 2.5% respectively, while O (0.6%) and S (2.7%) embrittle the GB. In Σ3, only C was found to strengthen the interface by 1.2%, while B, N, O, P and S decreases the intergranular fracture energy by 1.7, 1.6, 11.2, 18.4 and 19.4% respectively.

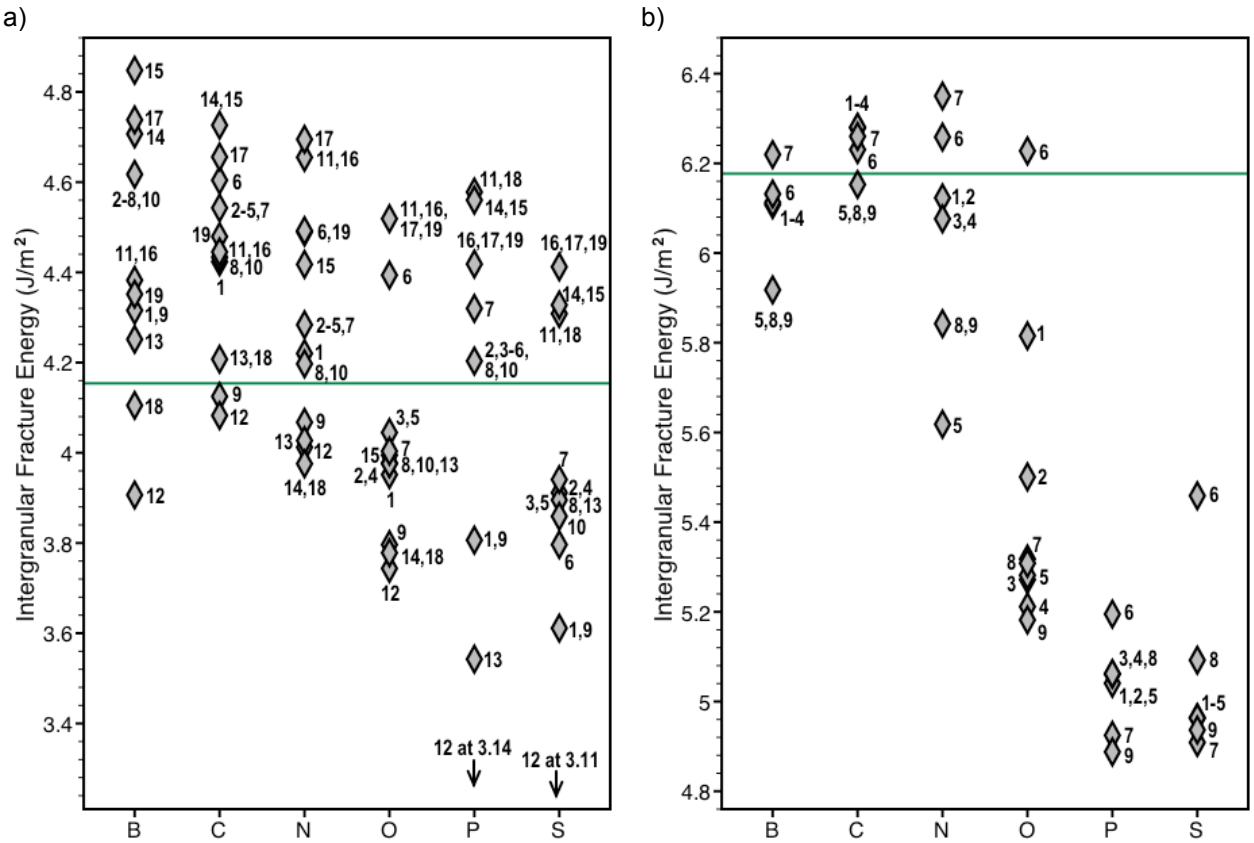

Figure 2. Intergranular fracture energy of a) W Σ27a{552} and b) W Σ3a{112} GBs with an impurity at various interstices. The lines at 4.16 and 6.18 J/m^2 mark the fracture energies of the pure GBs.

Table 3. Intergranular fracture energy change ΔE_{if} due to an impurity at various interstices in W Σ27{552} and Σ3{112} GBs. The minimum, maximum and average (bold face) values are given. The average effect was calculated using the segregation energy as a weighing factor. All values are normalized relative to the fracture energy of the clean interfaces and given in percentage. Positive numbers indicate an increased GB cohesion.

	B	C	N	O	P	S
Σ27	-5.9,16.7,**10.1**	-1.7,13.8,**8.9**	-4.3,13.0,**4.1**	-9.9,8.8,**-0.6**	-24.5,10.2,**2.5**	-25.2,6.2,**-2.7**
Σ3	-4.2,0.7,**-1.7**	-0.4,1.7,**1.2**	-9.0,2.8,**-1.6**	-16.1,0.8,**-11.2**	-20.9,-15.9,**-18.4**	-20.5,-11.6,**-19.4**

Computations were performed partly on Olympus supercomputer (FUSION account) at Pacific Northwest National.

REFERENCES

[1] Y. Mutoh, et al., *J. Mat. Sci.* **30** (1995) 770.
[2] S. Wurster, et al., *J. Nucl. Mater.* **413** (2011) 166.
[3] L. J. Kecskes, et al., *Mater. Sci. Eng. A* **467** (2007) 33.
[4] M. Faleschini, et al., *J. Nucl. Mater.* **367** (2007) 800.
[5] E. Lassner and W. -D. Schubert, “Tungsten”, Springer (1995).
[6] Y. Ishiyama, et al., *Mater. Sci. Eng. A* **473** (2008) 7.
[7] G. J. Ackland and R. Thetford, *Phil. Mag. A* **56** (1987) 15.
[8] P. E. Blöchl, *Phys. Rev. B* **50** (1994) 17953.
[9] G. Kresse and D. Joubert, *Phys. Rev. B* **59** (1999) 1758.
[10] J. P. Perdew, K. Burke, and M. Ernzerhof, *Phys. Rev. Lett.* **77** (1996) 3865.
[11] W. Setyawan and R. J. Kurtz, *Scrip. Mater.* **66** (2012) 558.